Stochastic quantification of the electric power generated by a piezoelectric energy harvester using a time–frequency analysis under non-stationary random vibrations

2014 Smart Mater. Struct. 23 045035

(http://iopscience.iop.org/0964-1726/23/4/045035)

IOP Publishing Smart Materials and Structures
Smart Mater. Struct. **23** (2014) 045035 (18pp) doi:10.1088/0964-1726/23/4/045035

Stochastic quantification of the electric power generated by a piezoelectric energy harvester using a time–frequency analysis under non-stationary random vibrations

Heonjun Yoon and Byeng D Youn

System Health and Risk Management Laboratory, Department of Mechanical and Aerospace Engineering, Seoul National University, Seoul, 151-742, Republic of Korea

E-mail: bdyoun@snu.ac.kr

Received 8 October 2013, revised 9 January 2014
Accepted for publication 27 January 2014
Published 10 March 2014

Abstract

Vibration energy, which is widely available, can be converted into electric energy using a piezoelectric energy harvester that generates alternating current in response to applied mechanical strain. For the last decade, there has been a strong surge of interest in developing an electromechanically-coupled analytical model of a piezoelectric energy harvester. Such a model is of great importance to enable understanding of the first principle of the piezoelectric transduction and to quantify harvestable electric power under a given vibration condition. However, existing analytical models that operate under an assumption of deterministic excitations cannot deal with the random nature present in realistic vibrations, even though this randomness considerably affects the variation in harvestable electric power. Furthermore, even when random vibrations are taken into account, existing stochastic analytical models can only be applied to stationary excitations, such as in the case of white Gaussian noise. This paper thus proposes a three-step framework for stochastic quantification of the electric power generated by a piezoelectric energy harvester under non-stationary random vibrations. First, we propose estimation of the time-varying power spectral density (PSD) of the input non-stationary random vibration using a statistical time–frequency analysis. The second step is to employ an existing electromechanical model as the linear operator for calculating the output voltage response. The final step is to estimate the time-varying PSD of the output voltage response. Following this three-step process, the expected electric power can be estimated from the autocorrelation function which is the inverse Fourier transform of the time-varying PSD of the output voltage response. The merits of the proposed framework are two-fold in that it enables: (i) quantification of the time-varying electric power generated under non-stationary random vibrations and (ii) consideration of the randomness in the design process of the energy harvester. Four case studies are used to demonstrate the effectiveness of the proposed framework.

Keywords: piezoelectric energy harvesting, analytical model, time–frequency analysis, non-stationary random vibrations, time-varying power spectral density

1. Introduction

Advances in wireless communications and low-power technology have enabled more widespread use of wireless sensor networks (WSNs). However, the limited life expectancy and high replacement cost of batteries still make it difficult to use wireless sensors, although they have many benefits over wired sensors. Energy harvesting (EH) technology, which scavenges electric power from ambient, otherwise wasted, energy sources, has been explored to develop self-powered

wireless sensors and possibly eliminate the battery replacement cost for wireless sensors [1–3]. Among ambient energy sources, vibration energy is one of the most widely available. Vibration energy can be converted into electric energy using piezoelectric [1, 3], electromagnetic [4, 5], electrostatic [6, 7], and/or magnetostrictive [8, 9] transduction mechanisms. Among the methods for vibration-based energy harvesting studied in the last decade, piezoelectric energy harvesting has been the preferred one due to its high energy density and the lack of need for external equipment. The transduction principle of a piezoelectric energy harvester is to generate alternating current (AC) in response to applied mechanical strain [10].

Piezoelectric energy harvesting requires multidisciplinary research. Extensive research effort has been made to advance the energy harvesting technology involving materials science, mechanical, and electrical engineering disciplines. It is never enough to emphasize only the material issues in order to improve the mechanical and electrical properties of piezoelectric materials. For example, piezoelectric ceramics, such as lead zirconate titanate (PZT), have the required high piezoelectric and dielectric constants, but are inherently brittle and not very durable. Meanwhile, piezoelectric polymers, such as a polyvinylidene fluoride (PVDF), have high flexibility but low electromechanical coupling. For this reason, many material scientists have worked to fabricate flexible as well as electromechanically efficient piezoelectric materials [11–13]. On the other hand, electrical regulation should be optimized to maximize the harvestable electric power, which is generally composed of three stages: (1) energy capture, (2) energy rectification, and (3) energy storage [14, 15]. One of the most important aspects in this electrical circuit configuration is the impedance matching between the piezoelectric energy harvester and the electrical regulation. Moreover, because a piezoelectric energy harvester produces alternating current (AC) in accordance with the sign change of the curvatures of the dynamic strains, an AC/DC converter is needed in order to use the harvested energy to operate electronic devices. From a mechanical perspective, a variety of design methodologies of mechanical characteristics have been proposed. For instance, shape optimization [16, 17] and topology optimization [18] have been implemented to enhance the generation of electric power. Furthermore, the importance of appropriate treatment of the flexible proof mass size has been suggested in micron-scale cantilever beam design due to its effect on the electromechanical performance [19]. Recently, nonlinear dynamics of bistable systems [20–22], resonance frequency tuning schemes [23, 24], and a multimodal resonator [25] have been proposed to reliably scavenge electric power under wideband vibrations. In particular, it has been proven that a segmentation design can achieve high electric power under broadband multiple vibration modes by removing piezoelectric materials to avoid voltage cancellation at strain nodes [10, 26]. Furthermore, as an alternative design paradigm of the cantilever beam, a commonly used piezoelectric energy harvester, a multifunctional energy harvesting skin (EH skin) has been proposed which can be directly attached to the surface of a vibrating engineered system and thus requires no clamping fixtures or proof mass [27, 28].

For the purpose of designing piezoelectric energy harvesters and selecting the best sites for installation, it is important to preliminarily quantify the harvestable electric power under a given vibration condition. An electromechanically-coupled analytical model of a piezoelectric energy harvester not only enables quick quantification of the harvestable electric power but also helps to provide information about important design considerations. In most cases, it is desirable to conduct this analytical approach prior to a computational or experimental one. Furthermore, the analytical approach is of great importance to understand the first principle of piezoelectric energy conversion and execute design optimization of a piezoelectric energy harvester in a cost-effective manner. Because of the great value of the analytical approach, many analytical models of a piezoelectric energy harvester have been developed to date with two primary distinct interests: (i) enhancement of the physics representation and (ii) consideration of the random nature in vibrations.

The first research interest attempts to provide models that better represent the physics of a piezoelectric energy harvester while assuming that the input vibration signal is a harmonic sinusoidal function. This research interest has driven development of two models: lumped- and distributed-parameter models. Round *et al* [29] developed a single degree of freedom lumped-parameter model for a cantilever beam; however, this model provides no dynamic strain distribution or modal analysis. Sodano *et al* [30] formulated a single degree of freedom model and studied electric charge performance. Because the lumped-parameter model might yield highly inaccurate results, Erturk *et al* [31] developed an amplitude correction factor which uses the ratio of tip mass to beam mass to accurately predict the voltage response of the lumped-parameter model. As an alternative modeling of a lumped-parameter model, DuToit *et al* [32] derived an approximate distributed-parameter model using the Rayleigh–Ritz discretization and a trial family of admissible functions. Kim *et al* [33] developed a rigorous modeling to investigate the effect of a proof mass which serves to decrease the resonance frequency and to raise the applied strain. Based on the Euler–Bernoulli beam theory, Erturk *et al* [34] proposed an electromechanically-coupled distributed-parameter model and verified its accuracy with experimental observations.

In practice, however, most realistic vibrations have physical uncertainty, such as variation of amplitude and driving frequency. Although this randomness considerably affects the variation in harvestable electric power, analytical models which operate under the assumption of deterministic excitations cannot deal with the random nature in realistic vibration signals. This drives the second research interest mentioned above, which is to analyze the amount of harvestable electric power of a piezoelectric energy harvester in a stochastic manner. There have been several attempts to develop an analytical model which accounts for random vibrations. In most existing stochastic models, it is assumed that the excitation is white Gaussian noise (WGN), which is wideband vibration and has a time-invariant power spectral density (PSD). Halvorsen [35] formulated a stochastic description using a PSD to calculate electric power, proof mass displacement, and optimal load

of resonant energy harvesters based on the Fokker–Plank equation. Adhikari *et al* [36] presented a closed form of a linear single degree-of-freedom model when the excitation is assumed to be white Gaussian noise. Seuaciuc-Osorio *et al* [37] investigated harvestable electric power from harmonic excitation with a sinusoidally varying driving frequency and constant amplitude. Ali *et al* [38] developed an equivalent linear model for piezo-magneto-elastic energy harvesters under broadband random vibrations. Zhao *et al* [39] predicted the expected electric power and mean-square shunted displacement based on a constant PSD by employing the Fourier series representation or an Euler–Maruyama scheme to solve the stochastic differential equations.

Even though several analytical models that account for random vibrations have been developed, existing models cannot be used to predict the amount of harvestable power under realistic, non-stationary vibration signals which have both random amplitude and frequency modulations. To address this challenge, this paper proposes a three-step framework for stochastic quantification of the electric power of a piezoelectric energy harvester under non-stationary random vibrations. To the best of our knowledge, this study is the first attempt to apply a statistical time–frequency analysis to electric power quantification of a piezoelectric energy harvester to deal with the non-stationary random nature of realistic vibrations.

The rest of this paper is organized as follows. Section 2 gives a brief review of the fundamentals of piezoelectricity and random vibrations. The proposed framework for stochastic quantification of harvestable electric power under non-stationary random vibrations is presented in section 3. Section 4 explains how to model the non-stationary random vibration signal and estimate the time-varying PSD of an input non-stationary random vibration using a statistical time–frequency analysis. An electromechanical model is briefly introduced as the linear operator for calculating the output voltage response in section 5. Section 6 explains how to estimate the time-varying PSD of the output voltage response. The effectiveness of the proposed framework is demonstrated using four case studies in section 7. Finally, the conclusion of this work is given in section 8.

2. Brief review of the fundamentals of piezoelectricity and random vibrations

To perform stochastic quantification of the electric power generated by a piezoelectric energy harvester under non-stationary random vibrations, two fundamental theories are required: (i) piezoelectricity and (ii) non-stationary random vibrations. To help the reader to better understand the proposed framework, this section gives a brief review of the fundamental theories of piezoelectricity and random vibrations.

2.1. Piezoelectricity

The prefix ‘piezo’ comes from the Greek ‘piezein’ which means to pressure or squeeze. Electricity is a physical phenomenon related to the flow of an electric charge. Therefore, piezoelectricity is ‘an interaction between electrical and mechanical behavior’ [40].

As a direct piezoelectric effect, a piezoelectric material can produce electric polarization due to applied mechanical strain. Piezoelectric energy harvesting and piezoelectric transducers correspond to this direct piezoelectric effect. The amount of voltage generated is proportional to the dynamic strain. Conversely, when electric polarization is applied, a piezoelectric material becomes strained. This is called the inverse piezoelectric effect.

In the IEEE Standard on Piezoelectricity (1987), the piezoelectric constitutive relations are given as [41]

$$T_{ij} = c^E_{ijkl} S_{kl} - e_{kij} E_k \tag{1}$$

$$D_{\mathrm{i}} = e_{ikl} S_{kl} - \varepsilon^S_{ij} E_k. \tag{2}$$

These expressions are also called the stress-charge form. In this case, the independent variables are the strain S_{kl} and electric field E_k. It should be noted that the elastic constant c^E_{ijkl} and dielectric permittivity ε^S_{ij} (also called the dielectric constant) are coupled to each other [42].

To calculate the electric current $i(t)$ in response to applied mechanical strain, Gauss’s law, also known as Gauss’s flux theorem, can be used with respect to the electric displacement D_{i} in an integral form as [43]

$$i(t) = \frac{\mathrm{d}}{\mathrm{d}t}(\Phi_{\mathrm{D}}) = \frac{\mathrm{d}}{\mathrm{d}t}\left(\int_A \boldsymbol{D}\cdot\boldsymbol{n}\,\mathrm{d}A\right) \tag{3}$$

where Φ_{D} is the electric displacement flux related to free charge. Because the unit vector $\boldsymbol{n}$ refers to the outward normal vector of the surface of the piezoelectric material, the direction of $(\boldsymbol{D}\cdot\boldsymbol{n})$ is determined in accordance with the poling direction.

2.2. Non-stationary random vibrations

A non-stationary random vibration signal can be considered as a one-dimensional stochastic process which refers to a family of random variables [44]. The possibility to mathematically describe the random nature of a realistic vibration signal depends on whether a stochastic process exhibits a statistical regularity or not [45]. If so, unlike a deterministic vibration signal, the behavior of a random vibration signal can be described in terms of statistical moments or probability density functions (PDFs) which contain meaningful information about the stochastic process.

Statistical moments can be computed over the entire collection of samples, resulting in what are called ensemble averages. As one of the ensemble averages, the autocorrelation function $R_X(t,\tau)$ of a vibration signal $x(t)$ can be defined as follows:

$$R_X(t,\tau) = E[x(t)x^*(t+\tau)] \tag{4}$$

where $E[\bullet]$ is the statistical expectation and τ is the time-lag. The physical meaning of the autocorrelation function of a vibration signal is ‘the degree of association of the signal at time t with itself at time $(t+\tau)$’ [46]. It can be also defined as the inverse Fourier transform of the time-varying PSD $S_X(t,\omega)$, as follows:

$$S_X(t,\omega) = \int_{-\infty}^{\infty} R_X(t,\tau)\mathrm{e}^{-\mathrm{i}\omega\tau}\mathrm{d}\tau. \tag{5}$$

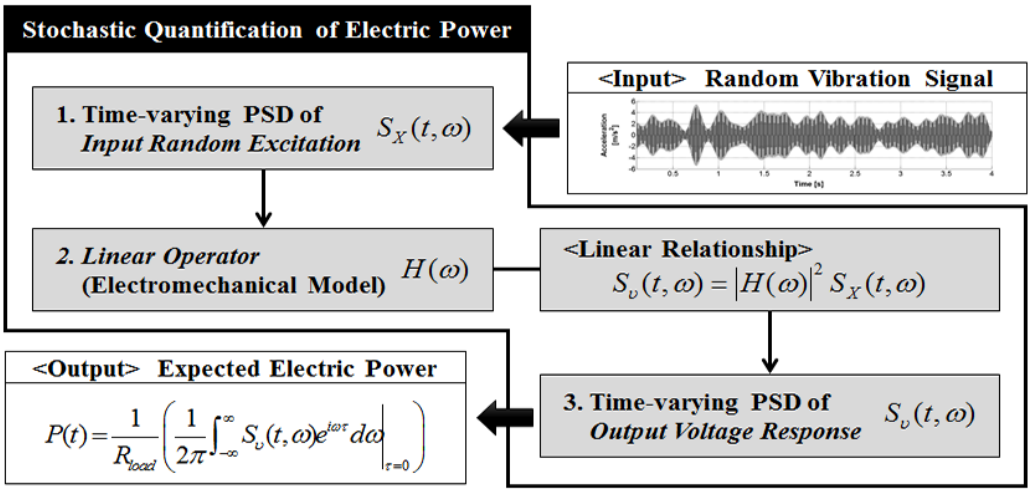

Figure 1. Framework for the stochastic quantification of the electric power generated by a piezoelectric energy harvester under non-stationary random vibrations.

The physical meaning of the time-varying PSD is that the local average power of the variance is decomposed in the time and frequency domains. As we can see from equation (5), when a random vibration signal is non-stationary, the stochastic process described in the frequency domain ω also depends on the time t. To characterize a non-stationary random vibration signal with time-varying amplitude and driving frequency, a statistical time–frequency analysis is needed, which can represent how the energy of the signal is distributed over both the time and frequency domains [47]. The time–frequency analysis can also identify the variation in frequency content with time; as a result, it is called the instantaneous frequency (IF). The details of the theory of random vibrations are explained in [48].

3. Framework for stochastic quantification of electric power under non-stationary random vibrations

As mentioned in section 1, the predictive capability of an analytical model is normally poor under random vibrations. Therefore, stochastic quantification of harvestable electric power should be able to systematically handle the random nature in realistic vibration signals of engineered systems. In this research, therefore, we propose a framework for stochastic quantification of the electric power produced by a piezoelectric energy harvester under non-stationary random vibration. The key new idea in this framework is a statistical time–frequency analysis, which is the first attempt to quantify the electric power generated by a piezoelectric energy harvester.

The proposed framework is composed of three sequentially executed procedures, as shown in figure 1. The first step is to estimate the time-varying PSD of the input non-stationary random vibrations $S_X(t,\omega)$. There are two main tasks in the first step: (i) mathematical modeling of the non-stationary random vibration signals and (ii) statistical time–frequency analysis to estimate the time-varying PSD. The second step of our approach is to employ an electromechanical model as the linear operator $H(\omega)$. In the proposed framework, the linear operator defines the linear relationship between the time-varying PSDs of the input non-stationary random vibrations and the output voltage response. The third step is to estimate the time-varying PSD of the output voltage response $S_\upsilon(t,\omega)$ from the linear relationship. After using our three-step approach, the expected electric power can be obtained from the autocorrelation function which is the inverse Fourier transform of the time-varying PSD of the output voltage response. Specific techniques and guidelines will be explained for each step in the following sections.

4. The time-varying power spectral density of non-stationary random vibrations

4.1. Mathematical modeling of non-stationary random vibrations

In most cases, variation of the operating conditions of a vibrating engineered system affect the statistics of the measured vibration signals over time [49]. This implies that most realistic vibration signals from engineered systems are inherently non-stationary. Therefore, unlike stationary vibrations, the mathematical description of non-stationary vibrations must be modeled as a function of time [50]. This mathematical representation can then be used to extract the physically meaningful information involved in signal realization based upon the acquired vibration data [51].

For several decades, many researchers have proposed mathematical representations of vibration signals, such as autoregressive (AR) [52–55], moving average (MA) [56], autoregressive moving average (ARMA) [57, 58], and empirical mode decomposition (EMD) [59–61]. In this study, an analytic non-stationary random vibration signal $x(t)$ is generated. Its mathematical description is decomposed by the combination of mono-component signals based on the concept of the Hilbert

transform as [62]

$$x(t) = \sum_{r}^{p} A_r(t) \cos\left[\int_0^t \omega_r(t)\mathrm{d}t\right] \tag{6}$$

where p is the number of mono-component signals, $A_r(t)$ is the instantaneous amplitude, and $\omega_r(t)$ is the instantaneous frequency of the rth mono-component signal. These instantaneous parameters are assumed to be slowly time-varying in a random manner. The instantaneous frequency is the first derivative of the instantaneous phase. In the case of a mono-component harmonic signal, the amplitude and the instantaneous frequency are constant, but the instantaneous phase increases linearly with time [62].

In general, vibrations can be measured in terms of displacement, velocity, or acceleration. In this paper, the vibration signal $x(t)$ in equation (6) is considered as an acceleration. Because poor quantification of electric power is mainly caused by variation of the driving frequencies and the peak amplitude levels of the acceleration signal, the amplitude and instantaneous frequency should be accurately localized using a time–frequency analysis.

4.2. Estimation of the time-varying PSD of non-stationary random vibration

This section explains how to estimate the time-varying PSD of an input non-stationary random vibration signal using a time–frequency analysis which can localize the frequency components of the vibration signal in both time and frequency domains. Time localization seeks to characterize a signal described during a time interval [63]. On the other hand, frequency localization seeks to identify the spectral components that are represented at particular frequencies [63]. Therefore, the choice of a time–frequency analysis plays an important role for accurate extraction of probabilistic information on a vibration signal. In the proposed framework, the Wigner–Ville spectrum, a bilinear time–frequency representation, is used to estimate the time-varying PSD of a non-stationary random vibration signal. Further discussion of the Wigner–Ville spectrum will be presented in the following section.

4.2.1. The Wigner–Ville spectrum. For localization of the instantaneous frequency of an amplitude modulation (AM) with the multiplicative noise and a linear frequency modulation (FM), the Wigner–Ville distribution (WVD) is known to be unbiased in estimation of the spread of signal energy in both the time and frequency domains [47]. The Wigner–Ville distribution is one of the most commonly used time–frequency analyses. The Wigner–Ville distribution is defined as [47]

$$\mathrm{WVD}_X(t,\omega) = \int_{-\infty}^{+\infty} x(t)x^*(t+\tau)\mathrm{e}^{-\mathrm{i}\omega\tau}\mathrm{d}\tau. \tag{7}$$

As mentioned in section 2.2, the time-varying PSD $S_X(t,\omega)$ is defined as the Fourier transform of the auto-correlation function $R_X(t,\tau)$; its form is similar to that of the Wigner–Ville distribution. Therefore, the time-varying PSD can be obtained from the ensemble averages of the Wigner–Ville distribution, the so-called Wigner–Ville spectrum, as [47]

$$\begin{aligned} S_X(t,\omega) &= \int_{-\infty}^{\infty} R_X(t,\tau)\mathrm{e}^{-\mathrm{i}\omega\tau}\mathrm{d}\tau \\ &= \int_{-\infty}^{\infty} E[x(t)x^*(t+\tau)]\mathrm{e}^{-\mathrm{i}\omega\tau}\mathrm{d}\tau \\ &= E\left[\int_{-\infty}^{\infty} x(t)x^*(t+\tau)\mathrm{e}^{-\mathrm{i}\omega\tau}\mathrm{d}\tau\right] \\ &= E[\mathrm{WVD}_X(t,\omega)]. \end{aligned} \tag{8}$$

However, it is extremely difficult to directly use the Wigner–Ville spectrum because ensemble averages demand a large number of signal realizations. Alternatively, if a stochastic process is stationary, ensemble averages that compute statistical moments over the entire collection of signals can be replaced by time averages that calculate statistical moments using only one representative signal over time. In this case, the stochastic process is said to be ergodic. Therefore, it is assumed that the Wigner–Ville distribution is locally ergodic in a smoothing kernel function $\Pi(t-u,\omega-v)$ so as to replace the ensemble averages with the time averages [47]. By taking the time averages of the Wigner–Ville distribution, we can estimate the time-varying PSD $\hat{S}_X^{\Pi}(t,\omega)$, which is the Wigner–Ville spectrum of non-stationary random vibrations, as [64]

$$\hat{S}_X^{\Pi}(t,\omega) = \iint_{-\infty}^{+\infty} \mathrm{WVD}_X(u,v)\Pi(t-u,\omega-v)\,\mathrm{d}u\,\mathrm{d}v. \tag{9}$$

Equation (9) is the same as in the case of the unified framework for Cohen's class, denoted by $C_X(t,\omega;\Pi)$ [65]. It can also be considered as two-dimensional convolution. There are two famous Wigner–Ville spectrum estimators: (1) the spectrogram and (2) the smoothed pseudo Wigner–Ville distribution (SPWVD). The spectrogram is defined as [47]

$$\begin{aligned} \hat{S}_{X,\mathrm{SPG}}^{g}(t,\omega) = \int_{-\infty}^{+\infty}\int_{-\infty}^{+\infty} &\mathrm{WVD}_X(\tau,v) \\ &\times\ g(\tau-t,v-\omega)\,\mathrm{d}\tau\,\mathrm{d}v. \end{aligned} \tag{10}$$

In the spectrogram, since only one smoothing window $g(\tau-t,v-\omega)$ is used in both time and frequency domains, the frequency can be smeared according to the Heisenberg–Gabor uncertainty principle which leads to a trade-off between time and frequency resolution [47]. In other words, the resolution cannot be simultaneously improved in both the time and frequency domains. For example, the shorter the size of the smoothing window in the time domain, the better the time resolution that can be achieved. However, the larger the spectrum bandwidth is, the poorer the frequency resolution is [66]. On the other hand, the SPWVD adjusts the time and frequency smoothing kernel functions separately, as [47]

$$\begin{aligned} \hat{S}_{X,\mathrm{SPWV}}^{g,h}(t,\omega) = \int_{-\infty}^{+\infty}\int_{-\infty}^{+\infty} &\mathrm{WVD}_X(\tau,v) \\ &\times\ g(\tau-t)h(v-\omega)\,\mathrm{d}\tau\,\mathrm{d}v. \end{aligned} \tag{11}$$

The use of separable kernel functions $g(\tau-t)$ and $h(v-\omega)$ allows control of the smoothing performance

in the time and frequency domains individually [64]. If a non-stationary random vibration signal is a multi-component frequency modulation, the smearing problem can be more serious due to the inherent characteristics of smoothing kernel functions. To improve the localization of the instantaneous frequency, one can use 'the reassignment technique which consists of a smoothing to reduce interferences and a squeezing to refocus components' [66]. This technique rearranges the values of the Wigner–Ville distribution 'not to the center of geometry but the center of mass in the smoothing window' by computing a centroid point as [47, 66]

$$\hat{t}(t,\omega) = t - \frac{\hat{S}^{t\cdot g,h}_{X,\mathrm{SPWV}}(t,\omega)}{\hat{S}^{g,h}_{X,\mathrm{SPWV}}(t,\omega)} \tag{12}$$

$$\hat{\omega}(t,\omega) = \omega + \mathrm{i}\frac{\hat{S}^{g,\mathrm{d}h/\mathrm{d}t}_{X,\mathrm{SPWV}}(t,\omega)}{\hat{S}^{g,h}_{X,\mathrm{SPWV}}(t,\omega)}. \tag{13}$$

As expected, the readability of the SPWVD is generally better than that of the spectrogram. In this study, the SPWVD was thus used for the purpose of demonstration in the case studies in section 7. Of course, as long as we appropriately choose any time–frequency analysis technique (e.g., evolutionary spectrum, Choi–Williams distribution, or wavelet transform) depending on a given vibration condition, the chosen technique can be implemented to estimate the time-varying PSD as well as the Wigner–Ville spectrum in the proposed framework.

4.2.2. Selection of the smoothing kernel functions. The resolvability of a vibration signal depends on not only the kind of time–frequency analysis but also the selection of a smoothing kernel function. Therefore, the appropriate shape and size of a smoothing window should be carefully selected for the optimal localization based on the characteristics of the vibration signals. In general, rectangular, Gauss, Hamming, Hanning, and Kaiser windows are used through a compromise between the smearing due to the main lobe and the leakage due to the side lobes caused by the convolution operation in the smoothing window [46].

For example, to resolve several closely spaced frequency components in the signal, a smoothing window having a narrow main lobe is suitable. Meanwhile, if the amplitude is more significant than the localization of a frequency component, a smoothing window having a wide main lobe is recommended [67]. On the other hand, if the interference terms (or cross-terms) which are a natural characteristic of bilinear time–frequency representations, such as the Wigner–Ville spectrum, are far from the frequency of interest, a smoothing window having a high roll-off rate of the side lobe is recommended. In contrast, if interference terms exist near the frequency of interest, a smoothing window having a low highest-side lobe is a good candidate [67]. In general, the Hanning window which has a moderate frequency resolution and good side lobe roll-off is acceptable in most cases [46]. Details about the effect of the smoothing window for signal processing are explained in [46, 67].

After determining the optimal size of the chosen smoothing window, the time-varying PSD of the input non-stationary random vibration signal is finally estimated. In the proposed framework, this time-varying PSD will be used as the input of a linear operator which will be defined in the following section for calculation of the time-varying PSD of the output voltage response.

5. Electromechanical model as the linear operator

One of the most important aspects in a stochastic process is to find the linear operator between the input excitation and the output response; this makes it possible to analytically obtain certain probabilistic information [68]. In the proposed framework, any electromechanically-coupled analytical model can be employed as the linear operator, as long as it can be expressed in the form of a frequency response function (FRF) for the output voltage response at arbitrary driving frequency ω. Therefore, the proposed framework can be applied not only to the beam but also to the plate theory-based model with any electrode configuration (e.g., stack, unimorph, or bimorph).

In this study, the distributed-parameter electromechanical model, established by Erturk *et al* [34], for a bimorph cantilever-type piezoelectric energy harvester was employed as the linear operator. This section briefly introduces the distributed-parameter electromechanical model and explains the physical interpretation of each parameter.

5.1. Mechanical equation of motion and modal analysis

A bimorph cantilever-type piezoelectric energy harvester is utilized in a 31-mode configuration in which the directions of applied stress and generated voltage are perpendicular to each other. It can be modeled as a thin Euler–Bernoulli beam which neglects the effects of rotary inertia and shear deformation [69]. In this case, the damped mechanical equation of motion is expressed by a fourth-order partial differential equation with two boundary conditions. For the boundary conditions, fixed at $x = 0$ and free at $x = 1$, the transverse deflection and its slope are zero at $x = 0$ and the bending moment and shear force are zero at $x = 1$. As a result, the characteristic equation is given as [69]

$$\cos(\lambda_n)\cosh(\lambda_n) + 1 = 0 \tag{14}$$

where λ_n is the eigenvalue of the nth mode. The nth mode shape $\psi_n(x)$ can be expressed as [69]

$$\begin{aligned}\psi_n(x) = &\left[\cos\left(\frac{\lambda_n x}{l}\right) - \cosh\left(\frac{\lambda_n x}{l}\right)\right] \\ &- \left[\frac{\cos(\lambda_n)+\cosh(\lambda_n)}{\sin(\lambda_n)+\sinh(\lambda_n)}\right] \\ &\times \left[\sin\left(\frac{\lambda_n x}{l}\right) - \sinh\left(\frac{\lambda_n x}{l}\right)\right]\end{aligned} \tag{15}$$

where l is the length of the piezoelectric energy harvester. The bending stiffness $Y_s I$ of a bimorph cantilever composite beam with three layers is [34]

$$Y_s I = \frac{2b}{3}\left[Y_s\left(\frac{h_s^3}{8}\right) + c_{11}^E\left\{\left(h_p + \frac{h_s}{2}\right)^3 - \frac{h_s^3}{8}\right\}\right] \tag{16}$$

where b is the width of the piezoelectric energy harvester, h_s is the thickness of the substrate, and h_p is the thickness of the piezoelectric layers. c_{11}^E is the elastic modulus of the piezoelectric layers. The nth natural frequency ω_n can be calculated as [69]

$$\omega_n = \lambda_n^2 \sqrt{\frac{Y_s I}{m l^4}} \tag{17}$$

where m is the mass of the piezoelectric energy harvester. Since the mode shapes obtained from the boundary value problem are orthogonal, the expansion theorem can be used to describe the relative displacement $w_{rel}(x,t)$ of the piezoelectric energy harvester as [45]

$$w_{rel}(x,t) = \sum_{n=1}^{\infty} \psi_n(x)\eta(t) \tag{18}$$

where $\eta(t)$ is the modal mechanical response. In the Sturm–Liouville problem, because the sets of the orthogonal mode shapes $\psi_n(x)$ are complete in $L_2(0,l)$ space, the relative displacement absolutely and uniformly converges in the series of mode shapes [70].

Finally, the mechanical equation of motion in modal coordinates can be expressed as [34]

$$\frac{\partial^2 \eta(t)}{\partial t^2} + 2\zeta_n \omega_n \frac{\partial \eta(t)}{\partial t} + \omega_n^2 \mu(t) - \boldsymbol{\theta}_n \upsilon(t) = f(t) \tag{19}$$

where ζ_n is the modal damping. The electromechanical coupling $\boldsymbol{\theta}_n$, related to the energy conversion efficiency, is expressed as [34]

$$\boldsymbol{\theta}_n = \bar{e}_{31} \left(\frac{h_p + h_s}{2} \right) \left. \frac{\mathrm{d}\psi_n(x)}{\mathrm{d}x} \right|_{x=l}. \tag{20}$$

5.2. Electrical circuit equation

Since the poling direction of the bimorph cantilever piezoelectric energy harvester is normal to the top surface of the piezoelectric layer, the scalar product of the electric displacement $\boldsymbol{D}$ and the outward normal unit vector $\boldsymbol{n}$ in Gauss's law becomes D_3 as

$$i(t) = \frac{\mathrm{d}}{\mathrm{d}t} \left(\int_A \boldsymbol{D} \cdot \boldsymbol{n} \, \mathrm{d}A \right) = \frac{\mathrm{d}}{\mathrm{d}t} \left(\int_A D_3 \, \mathrm{d}A \right). \tag{21}$$

As a result, the electrical circuit equation can be derived by substituting the piezoelectric constitutive relation in equation (2) into equation (21) as [34]

$$\frac{\mathrm{d}}{\mathrm{d}t} \left(\int_A D_3 \, \mathrm{d}A \right) = \frac{\mathrm{d}}{\mathrm{d}t} \left\{ \int_A (\bar{e}_{31} S_1 + \varepsilon_{33}^S E_3) \, \mathrm{d}A \right\} \tag{22}$$

where $\bar{e}_{31}$ is the piezoelectric constant, ε_{33}^S is the dielectric permittivity at constant strain, and E_3 is the electric field. The dynamic strain S_1 can be expressed with respect to the neutral axis as

$$S_1 = -\left(\frac{h_p + h_s}{2} \right) \frac{\partial^2 w_{rel}(x,t)}{\partial x^2}. \tag{23}$$

Finally, the electrical circuit equation can be obtained as [34]

$$\frac{\upsilon(t)}{R_{load}} = -\bar{e}_{31} b \left(\frac{h_p + h_s}{2} \right) \int_0^l \left\{ \frac{\partial^3 w_{rel}(x,t)}{\partial x^2 \partial t} \right\} \mathrm{d}x - \frac{\varepsilon_{33}^S bl}{h_p} \left(\frac{\mathrm{d}\upsilon(t)}{\mathrm{d}t} \right) \tag{24}$$

where $\upsilon(t)$ is the output voltage and R_{load} is the external load.

By substituting equations (18) and (20) into equation (24), the electrical circuit equation can be expressed in modal coordinates as [34]

$$C_p \dot{\upsilon}(t) + \frac{\upsilon(t)}{R_{load}} + \sum_{n=1}^{\infty} \boldsymbol{\theta}_n \dot{\eta}(t) = 0 \tag{25}$$

where C_p is the capacitance of the piezoelectric energy harvester as follows:

$$C_p = \frac{\varepsilon_{33}^S bl}{h_p}. \tag{26}$$

5.3. Steady-state voltage response

Finally, the steady-state voltage response $\upsilon(\omega)$ can be obtained by simultaneously solving the mechanical equation of motion and the electrical circuit equation, as [71]

$$\upsilon(\omega) = \frac{\sum_{n=1}^{\infty} \frac{\mathrm{i}\omega R_{load} \boldsymbol{\theta}_n}{\omega_n^2 - \omega^2 + \mathrm{i}2\zeta_n \omega_n \omega}}{\left(\frac{1}{R_{load}} + \mathrm{i}\omega \frac{C_p}{2} \right) + \sum_{n=1}^{\infty} \frac{\mathrm{i}\omega R_{load} \boldsymbol{\theta}_n^2}{\omega_n^2 - \omega^2 + \mathrm{i}2\zeta_n \omega_n \omega}}. \tag{27}$$

In the proposed framework, this steady-state voltage response $\upsilon(\omega)$ is implemented as the linear operator $H(\omega)$. As the impedance matching for the maximum electric power, the optimal external load at the short-circuit resonance frequency can be obtained by setting

$$\frac{\partial \left[\frac{\upsilon(\omega)^2}{R_{load}} \right]}{\partial R_{load}} = 0. \tag{28}$$

As a result, the optimal external load for the short-circuit resonance frequency is expressed as [71]

$$R_{load}^{\mathrm{opt},\omega_n^{sc}} = \frac{1}{\omega_n C_p \left[1 + \left\{ \frac{\bar{e}_{31} b (h_p + h_c)}{4\zeta_n^2} \left(\left. \frac{\mathrm{d}\psi_n(x)}{\mathrm{d}x} \right|_{x=l} \right) \right\}^2 \right]^{1/2}}. \tag{29}$$

According to equation (29), the optimal external load only depends on the mechanical (e.g., natural frequency, mode shape, geometry, and damping ratio) and electrical (e.g., piezoelectric constant and capacitance) parameters of the piezoelectric energy harvester. This means that the optimal external load does not depend on the given vibration condition, if the driving frequency of the vibrating engineered system is adjacent to the resonance frequency. Therefore, the optimal external load, derived under the assumption of deterministic excitation, can also be used under non-stationary random vibrations.

6. Time-varying power spectral density of the output voltage response

In this section, we estimate the time-varying PSD of the output voltage response from the linear relationship. As mentioned in section 2.2, the autocorrelation function of a vibration signal can be obtained by computing the inverse Fourier transform of its time-varying PSD. Finally, based on the definition of the autocorrelation function, the expected electric power can be quantified as a function of time. Detailed procedures will be explained in the following sections.

6.1. Estimation of the time-varying PSD of the output voltage response

Because of uncertainty propagation [72–74], 'if the input excitation is the stochastic process, the output response is also the stochastic process' [68]. As a stochastic dynamic, the linear relationship is then expressed in terms of a statistical moment, such as a time-varying PSD, as

$$S_\upsilon(\omega, t) = |H(\omega)|^2 S_X(\omega, t) + S_\mathrm{e}(\omega, t). \tag{30}$$

Therefore, the time-varying PSD $S_\upsilon(\omega, t)$ of the output voltage response can be estimated from the linear relationship between the input and output time-varying PSDs.

In the case of an impulsive response, the error $S_\mathrm{e}(\omega, t)$ involved in the approximation of the linear relationship for a vibrating system with high damping is smaller than that with low damping [75]. Since a piezoelectric energy harvester is generally manufactured as a highly resonant system with low damping, one can suppose that equation (30) is not valid. However, in the case that the piezoelectric energy harvester is continuously excited by forced vibrations from the surface of an engineered system, the error approaches zero as the time t increases. Therefore, given sufficient time, the error can be negligibly small and the assumption of a linear relationship is reasonable to estimate the time-varying PSD of the output voltage response.

6.2. Quantification of the expected electric power

As previously explained in section 2.2, the autocorrelation function $R_\upsilon(t, \tau)$ of the output voltage response $\upsilon(t)$ can be obtained by the inverse Fourier transform of the time-varying PSD $S_\upsilon(\omega, t)$ of the output voltage response as

$$R_\upsilon(t, \tau) = E[\upsilon(t)\upsilon(t+\tau)] = \frac{1}{2\pi}\int_{-\infty}^{\infty} S_\upsilon(\omega, t)\mathrm{e}^{\mathrm{i}\omega\tau}\mathrm{d}\omega. \tag{31}$$

In the end, the expected electric power $E[P(t)]$ can be obtained by dividing the autocorrelation function of the output voltage response by the external load R_load and taking zero time-lag ($\tau = 0$) as [36, 71]

$$E[P(t)] = \frac{E[\upsilon(t)^2]}{R_\mathrm{load}} = \frac{1}{2\pi R_\mathrm{load}}\int_{-\infty}^{\infty} S_\upsilon(\omega, t)\mathrm{e}^{\mathrm{i}\omega\tau}\mathrm{d}\omega\Big|_{\tau=0}. \tag{32}$$

Because the expected electric power quantified by the proposed framework is a function of time, it is possible to quickly visualize the variation of harvestable electric power over time based on the ambient vibration data acquired from the engineered system. This benefit again suggests that the proposed framework plays an essential role in scheduling the operation time interval (OTI) of wireless sensors when the amount of harvestable electric power is larger than the threshold at which it is set to activate their operation. Therefore, the proposed framework can be used to quickly confirm whether it is feasible or not to operate wireless sensor networks for structural health monitoring or building automation under a given vibration condition.

7. Case studies

This section uses four case studies to demonstrate the effectiveness of the proposed framework for stochastic quantification of the electric power of a piezoelectric energy harvester. In the first three case studies, different analytic non-stationary random vibration signals are described with the aim of investigating the effect of the randomness of the amplitude and driving frequency on the amount of harvestable electric power. The first case considers only variation of the amplitude, while the second case focuses on randomness of the driving frequency. The third case accounts for the combined effect of random variation of the amplitude and driving frequency simultaneously. For the purpose of comparing the proposed framework with a published stochastic electromechanical model, the last case study considers stationary white Gaussian noise (WGN).

7.1. Random amplitude and constant driving frequency

We first consider the following analytic vibration signal $x(t)$ with a random amplitude and constant driving frequency:

$$x(t) = \{A_\mathrm{c} + \sigma(t)\}\cos(2\pi f_\mathrm{c} t). \tag{33}$$

As mentioned in section 4.1, the analytic vibration signal with a random amplitude modulated by white Gaussian noise was generated based on the Hilbert transform, as shown in figure 2. The driving frequency f_c was 115 Hz but the amplitude was randomly modulated by the white Gaussian noise $\sigma(t)$ with a standard deviation of 0.357 m s^{-2}. The mean value A_c of the random amplitude was 4.905 m s^{-2} (0.5 g). This type of the vibration signal can be observed on a power transformer which is one of the most important engineered systems in a power plant. A power transformer operates at a fixed driving frequency, while the vibration amplitude of its core and winding is time-variant.

Because the root mean square (RMS) level of the vibration signal randomly changes with time, the traditional PSD cannot be identified in the frequency domain. Therefore, a time–frequency analysis is required to estimate the time-varying PSD of non-stationary random vibrations.

The proposed framework was applied to quantify the harvestable electric power under the given vibration condition. First, the time-varying PSD $S_X(\omega, t)$ of the input non-stationary random vibration signal with random amplitude

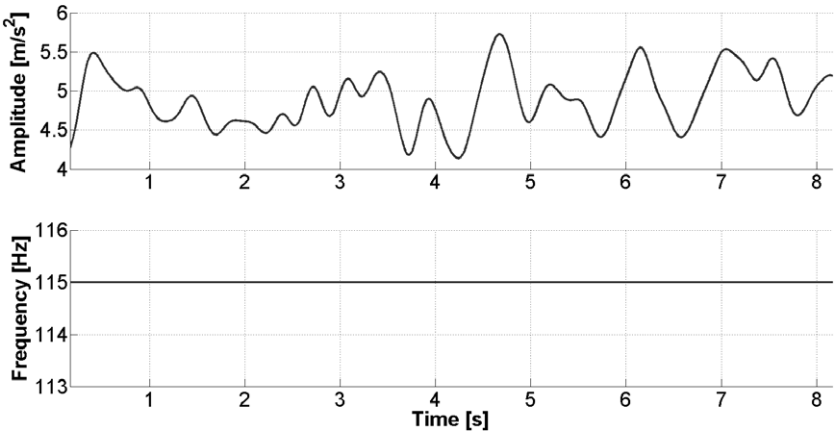

Figure 2. Decomposition of the non-stationary random vibration signal with random amplitude and constant driving frequency.

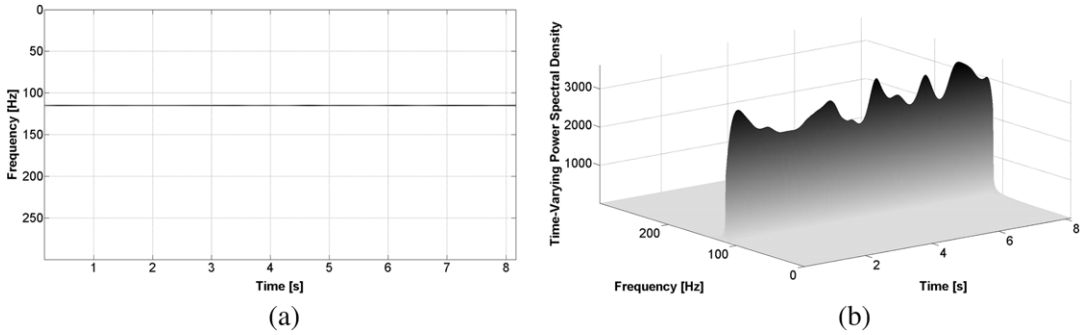

Figure 3. The time-varying power spectral density of the input non-stationary random vibration signal with random amplitude and constant driving frequency: (a) two-dimensional view; (b) three-dimensional view.

Table 1. The mechanical and electrical parameters of a commercially available bimorph cantilever-type piezoelectric energy harvester.

Mechanical parameters		Electrical parameters	
Elastic modulus of PSI-5H4E, c_{11}^E	66 GPa	Piezoelectric strain coefficient, d_{31}	-3.20×10^{-10} m V^{-1}
Elastic modulus of substrate, Y_s	124 GPa	Piezoelectric constant, $\bar{e}_{31}$	-21.12 C m^{-2}
Thickness of PSI-5H4E, h_p	0.2667 mm	Absolute permittivity, ε_0	8.85×10^{-12} F m^{-1}
Thickness of substrate, h_s	0.1016 mm	Dielectric permittivity at constant stress, ε_{33}^T	30.10×10^{-9} F m^{-1}
Density of PSI-5H4E, ρ_p	7500 kg m^{-3}	Dielectric permittivity at constant strain, ε_{33}^S	23.35×10^{-9} F m^{-1}
Density of substrate, ρ_s	7800 kg m^{-3}	Relative dielectric constant, ε_r	3400
Damping ratio, $\zeta_{n=1}$	0.0167	Capacitance, C_p	71.40×10^{-9} F
Length of energy harvester, l	0.0513 m	Electromechanical coupling, $\boldsymbol{\theta}_{n=1}$	6.60×10^{-3} N m^{-1}
Width of energy harvester, b	0.0318 m	Optimal impedance, $R_{\text{load}}^{\text{opt},\omega_n^{\text{sc}}}$	4190 Ω

and a constant driving frequency was estimated using the SPWVD. This study used separate Hanning windows for time and frequency smoothing. This is why the Hanning window is generally suitable for spectral analysis of random vibrations or noise measurements. The sizes of the Hanning window were 15 points in time and 1001 points in frequency, respectively.

Figure 3 shows the time-varying PSD of the input non-stationary random vibration signal with random amplitude and constant driving frequency in figure 2. Because the driving frequency was constant, the instantaneous frequency was localized on the 115 Hz line. Therefore, the magnitude of the time-varying PSD of the input non-stationary random vibration signal depends only on the amplitude of the acceleration.

In the second step, the linear operator $H(\omega)$ was calculated using the material properties of PZT-5H [76], as shown in table 1. The fundamental natural frequency was calculated as 115.47 Hz from equation (17) and the optimal external load for

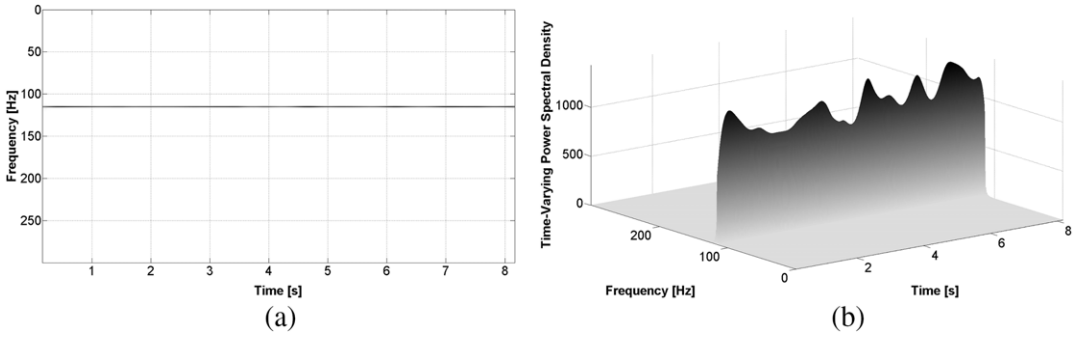

Figure 4. The time-varying power spectral density of the output voltage response under the non-stationary random vibration signal with random amplitude and constant driving frequency: (a) two-dimensional view; (b) three-dimensional view.

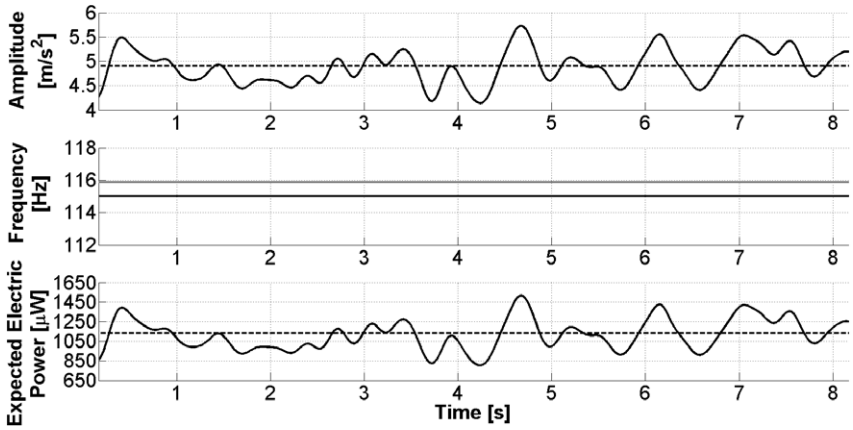

Figure 5. Expected electric power under the non-stationary random vibration signal with random amplitude and constant driving frequency.

the short-circuit resonance frequency was obtained as 4190 Ω from equation (29).

In the third step, the time-varying PSD $S_v(\omega, t)$ of the output voltage response was estimated from the linear relationship, as shown in figure 4.

Figure 5 shows the result of quantification of the expected electric power under a non-stationary random vibration signal with random amplitude and a constant driving frequency. In the frequency versus time plot, the upper solid line (gray) indicates the short-circuit resonance frequency of 115.9 Hz, while the lower solid line (black) describes the instantaneous frequency. The maximum expected electric power was approximately 1518 μW when the maximum acceleration amplitude was 5.729 m s^{-2} and when the driving frequency was 115 Hz at $t = 4.673$ s. It is worth noticing that the correlation coefficient of the amplitude and expected electric power was calculated as 0.9988. This strong correlation clearly shows that the amplitude of the input random vibration signal and the output electric power have the same phase, as shown in figure 5. This is why the amount of electric power generated by a piezoelectric energy harvester is generally proportional to the square of the acceleration amplitude at the same driving frequency.

In figure 5, the dashed line indicates a harvestable electric power of 1130.99 μW which was calculated in a deterministic manner under forced harmonic vibration with a constant amplitude of 4.905 m s^{-2} and driving frequency of 115 Hz. By comparing the results for electric power, it can be concluded that the proposed framework can assist one in more accurately calculating the harvestable electric power than a rough estimation obtained by assuming a constant amplitude and driving frequency under non-stationary random vibrations.

7.2. Constant amplitude and random driving frequency

Let us now consider the following analytic vibration signal with a random driving frequency and constant amplitude:

$$x(t) = A_c \cos\left[\int_0^t \{(2\pi f_c) + \varepsilon(t)\}\, dt\right]. \tag{34}$$

As shown in figure 6, the amplitude A_c was fixed at 4.905 m s^{-2}. The driving frequency was randomly modulated by Gaussian noise $\varepsilon(t)$ with a standard deviation of 0.63 Hz. The mean value f_c of the random driving frequency was 115 Hz. This kind of vibration signal can be observed in gearboxes where the gear mesh frequency changes when the gear changes its revolutions per minute (RPM).

In the first step, the time-varying PSD $S_X(\omega, t)$ of the input non-stationary random vibration signal with a random driving frequency and constant amplitude was estimated using the SP-WVD, as shown in figure 7. Separate Hanning windows were employed for each time smoothing and frequency smoothing in the SPWVD. The sizes of the Hanning windows were 15 points

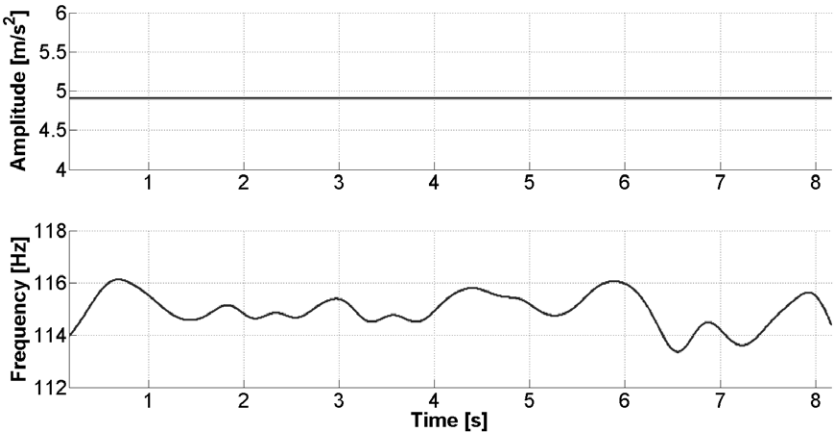

Figure 6. Decomposition of the non-stationary random vibration signal modulated with random driving frequency and constant amplitude.

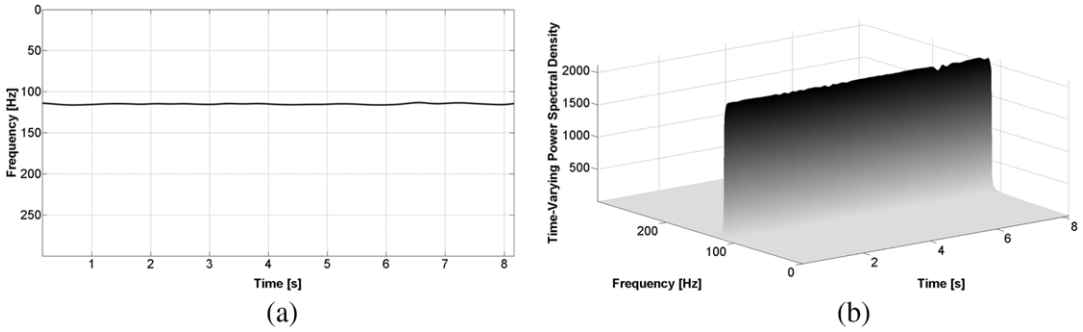

Figure 7. The time-varying power spectral density of the input non-stationary random vibration signal with random driving frequency and constant amplitude: (a) two-dimensional view; (b) three-dimensional view.

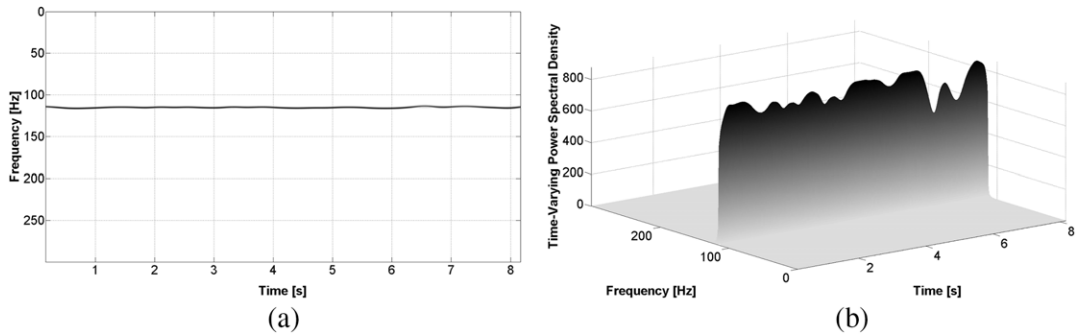

Figure 8. The time-varying power spectral density of the output voltage response under the non-stationary random vibration signal with random driving frequency and constant amplitude: (a) two-dimensional view; (b) three-dimensional view.

in time and 701 points in frequency, respectively. Figure 7(a) shows that the localized value of the instantaneous frequency randomly changes with time. However, the magnitude of the time-varying PSD of the input vibration signal is constant because the amplitude of the vibration signal is fixed over the entire time domain, as shown in figure 7(b).

Just like the first case study, the mechanical and electrical parameters of a commercially available piezoelectric energy harvester, which are summarized in table 1, were used to calculate the linear operator in the second step.

Finally, the time-varying PSD $S_v(\omega, t)$ of the output voltage response was estimated in the third step, as shown in figure 8. We note that the magnitude of the time-varying PSD of the output voltage response depends only on the variation of the instantaneous frequency. As shown in figure 8, the magnitude of the time-varying PSD of the output voltage response fluctuates, in contrast with that of the input vibration signal. This is why most vibration-based energy harvesters, such as piezoelectric energy harvesters, are designed as resonators. In other words, if the other conditions are the same, maximum voltage generation can be achieved when the resonance frequency matches the dominant excitation frequency of the ambient vibrations; so-called frequency matching. Figure 8 shows that the larger the difference between the instantaneous

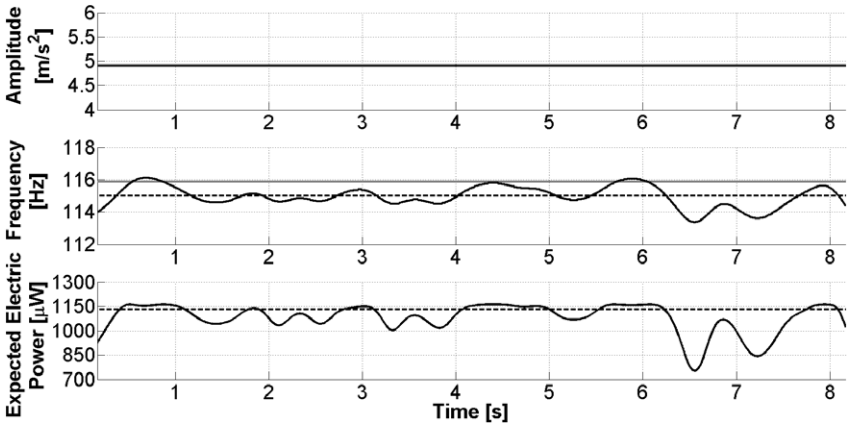

Figure 9. Expected electric power under the non-stationary random vibration signal with random driving frequency and constant amplitude.

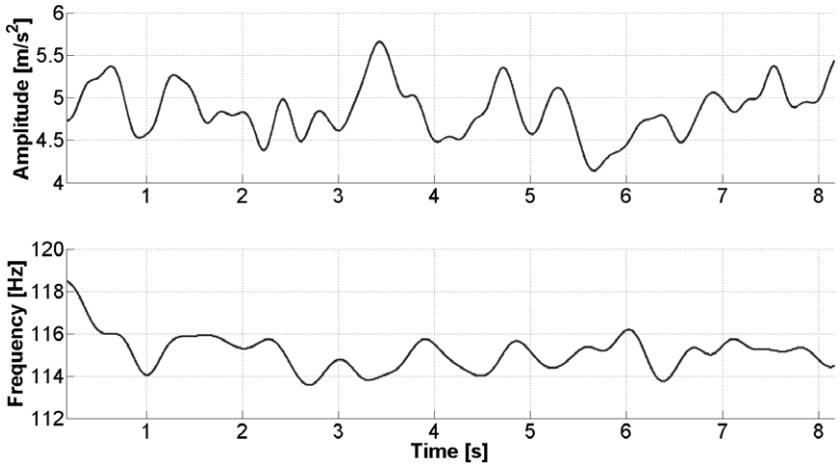

Figure 10. Decomposition of the non-stationary random vibration signal with random amplitude and driving frequency.

and resonance frequencies is, the lower the magnitude of the time-varying PSD of the output voltage response is.

This physical feature can be also confirmed through the result of stochastic quantification of the electric power, as shown in figure 9. For example, when the amplitude is constant at 4.905 m s^{-2}, a minimum electric power of 753.51 μW is generated at 113.34 Hz which is the farthest from the short-circuit resonance frequency of 115.9 Hz at $t = 6.555$ s. The window size in this case study is shorter than that of the first case study in the frequency domain for the purpose of reducing interference induced by variation of the driving frequency. As a result, the local extremes of the expected electric power might be slightly underestimated because greater frequency smoothing can reduce the peak values of the time-varying PSD.

7.3. Random amplitude and random driving frequency

The third case study considers the following analytic vibration signal with random amplitude and random driving frequency:

$$x(t) = \{A_c + \sigma(t)\} \cos\left[\int_0^t \{(2\pi f_c) + \varepsilon(t)\}\, dt\right]. \qquad (35)$$

As shown in figure 10, the amplitude was randomly modulated by Gaussian noise $\sigma(t)$ with a standard deviation of 0.31 m s^{-2}. The mean value A_c of the random amplitude was 4.905 m s^{-2}. The driving frequency was also modulated by Gaussian noise $\varepsilon(t)$ with a standard deviation of 0.82 Hz. The mean value f_c of the random driving frequency was 115 Hz.

Just like the previous two case studies, separate Hanning windows were used in the first step for time and frequency smoothing in the SPWVD. Their sizes were 15 points and 501 points, respectively. As a result, the time-varying PSD of the input non-stationary random vibration signal was estimated, as shown in figure 11.

Figure 12 shows the time-varying PSD $S_v(\omega, t)$ of the output voltage response. Note that even though the amplitude of the input non-stationary random vibration signal is high at a certain time, the magnitude of the time-varying PSD of the output voltage response can be relatively low when the instantaneous frequency is far from the short-circuit resonance frequency.

These characteristics of piezoelectric energy harvesting can also be ascertained from the result of the expected electric power under a non-stationary random vibration signal

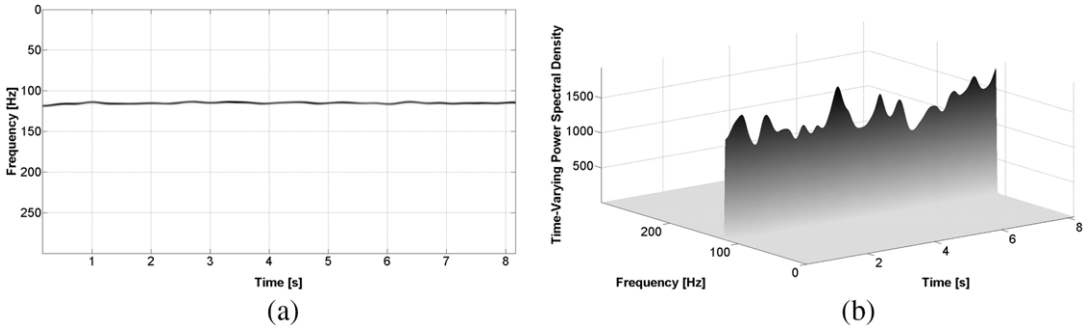

Figure 11. The time-varying power spectral density of the input non-stationary random vibration signal with random amplitude and driving frequency: (a) two-dimensional view; (b) three-dimensional view.

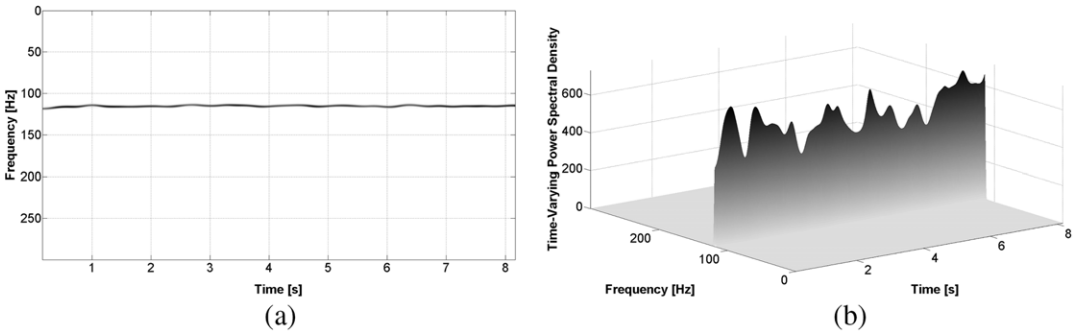

Figure 12. The time-varying power spectral density of the output voltage response under the non-stationary random vibration signal with random amplitude and driving frequency: (a) two-dimensional view; (b) three-dimensional view.

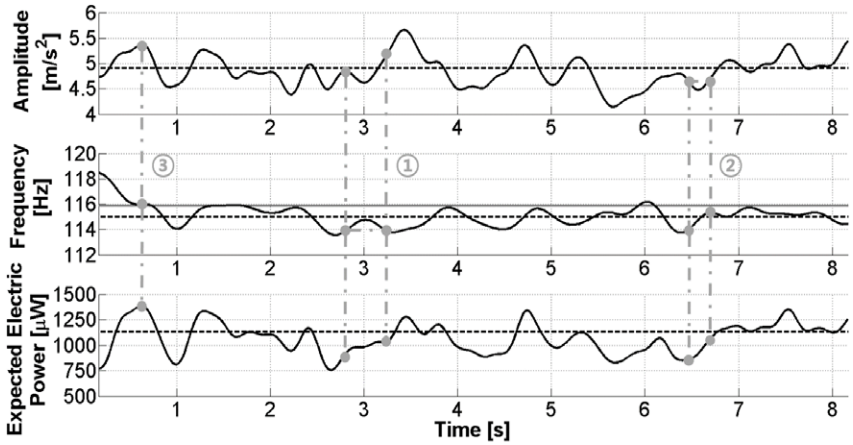

Figure 13. Expected electric power under the non-stationary random vibration signal with random amplitude and driving frequency.

with random amplitude and driving frequency, as shown in figure 13.

This result clearly illustrates that a larger amplitude and a closer distance between the instantaneous and short-circuit resonance frequencies ensures a higher expected generation of electric power. For instance, case ① in figure 13 indicates the effect of amplitude variation on harvestable electric power, while case ② examines the effect of frequency variation. Lastly, case ③ indicates the maximum expected electric power, which was approximately 1384.78 μW when the amplitude was 5.372 m s^{-2} (relatively high magnitude) and the instantaneous frequency was 115.98 Hz (frequency matching) at $t = 0.627$ s.

7.4. White Gaussian noise

The proposed framework is also applicable to stationary random vibrations. A typical example of stationary random vibrations is white Gaussian noise (WGN) which is a wideband random process and has a time-invariant PSD. As mentioned in section 1, there are several stochastic electromechanical models for calculating the expected electric power under

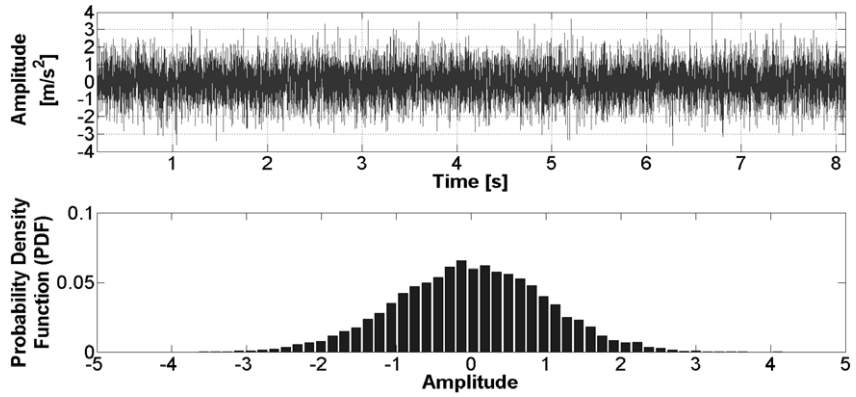

Figure 14. White Gaussian noise and its probability density function.

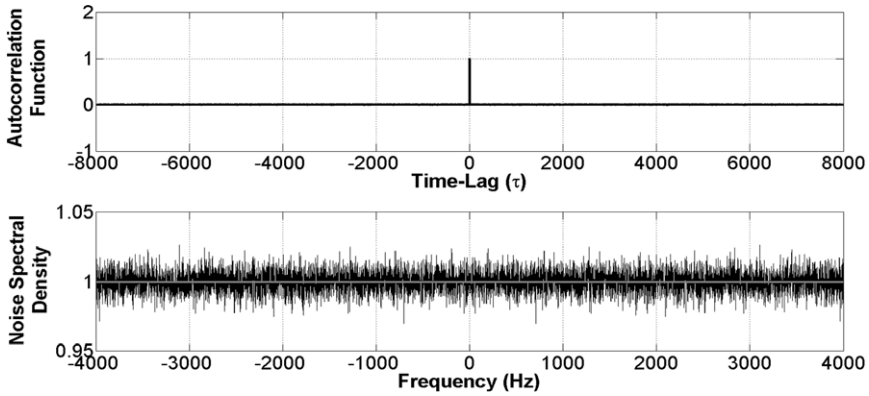

Figure 15. The autocorrelation function and two-sided noise spectral density of white Gaussian noise.

stationary WGN [35, 36, 39]. Therefore, for the purpose of comparing the proposed framework with a published stochastic electromechanical model, the last case study considers stationary WGN with zero mean and unit variance, as shown in figure 14.

Figure 15 shows the autocorrelation function, which is a Dirac delta function, and the noise spectral density of the WGN which is defined as the noise power per unit bandwidth. Even though ideal WGN has a constant noise spectral density theoretically, the limited bandwidth in practical implementation can cause deviation of the noise spectral density. The mean value of the noise spectral density was calculated as 1.0001 $m^2\ s^{-4}\ Hz^{-1}$ over the entire bandwidth.

The proposed framework uses the pseudo-excitation method [68] to estimate the PSD of WGN. A high sampling frequency is preferred in order to cover as wide a bandwidth as possible to be close to ideal WGN. In this study, the sampling frequency was 10 kHz. Because the magnitude of the PSD in figure 16 is the same as the product of the noise spectral density and the bandwidth, the PSD can be referred to as the power spectrum (PS). As shown in figure 16, the PSD of WGN is spread over the entire frequency bandwidth. We again note that the PSD of WGN is not a function of time.

From the linear relationship between the input and output PSDs, equation (30), the PSD of the output voltage response under the WGN was estimated as shown in figure 17.

Table 2. Expected electric power under stationary white Gaussian noise with zero mean and unit variance.

Quantification method	Expected electric power
Proposed framework	1142.86 μW (mean value)
Published stochastic electromechanical model [39]	1148.31 μW (mean value)

Figure 18 and table 2 show that the result of the expected electric power quantified by the proposed framework is in good agreement with that by the published stochastic electromechanical model established by Zhao and Erturk [39], under WGN with zero mean and unit variance. Therefore, it can be concluded from this observation that the proposed framework can be used as a generic method for calculating the expected electric power generated by a piezoelectric energy harvester under stationary as well as non-stationary random vibrations. The difference between the mean values of the expected electric power is about 5.5 μW. The difference can be explained by two different bandwidth ranges. The proposed framework quantifies the expected electric power over a limited bandwidth (one half of the Nyquist frequency), while the published stochastic electromechanical model calculates the analytical solution of the expected electric power over an infinite frequency range.

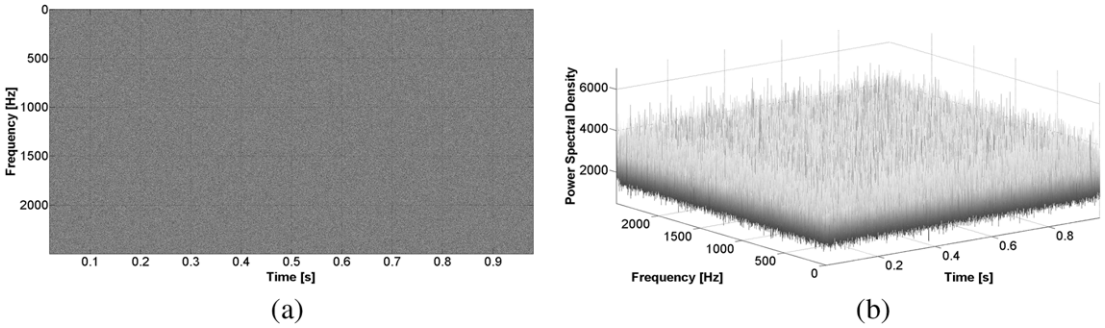

Figure 16. The power spectral density of white Gaussian noise: (a) two-dimensional view; (b) three-dimensional view.

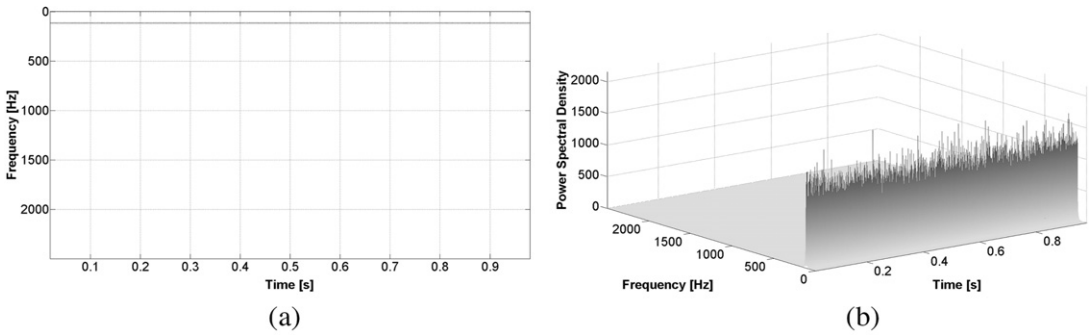

Figure 17. The power spectral density of the output voltage response under white Gaussian noise: (a) two-dimensional view; (b) three-dimensional view.

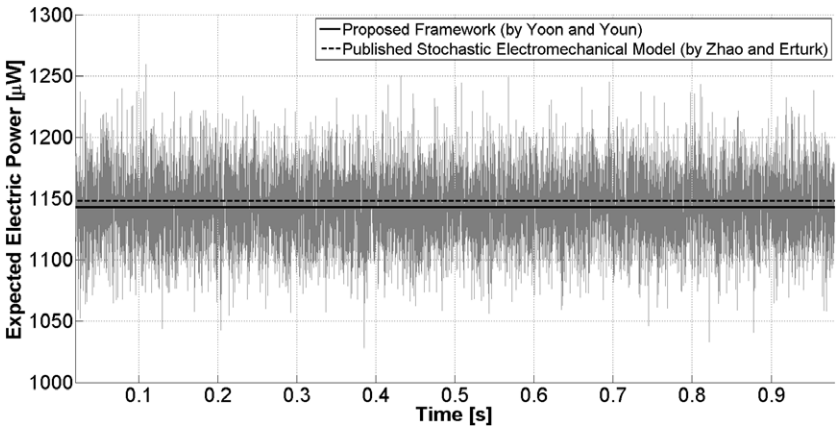

Figure 18. Comparison between the expected electric power results quantified by the proposed framework and a published stochastic electromechanical model [39] under stationary white Gaussian noise.

8. Conclusions

This paper proposed a three-step framework for stochastic quantification of the electric power generated by a piezoelectric energy harvester under non-stationary random vibrations. The sequentially executed procedures are summarized as follows.

- Step 1-1: mathematically represent the non-stationary random vibration signals.
- Step 1-2: estimate the time-varying PSD of the input non-stationary random vibrations using equation (11).
- Step 2: employ an electromechanical model as a linear operator using equation (27).
- Step 3-1: estimate the time-varying PSD of the output voltage response using equation (30).
- Step 3-2: obtain the expected electric power from the autocorrelation function which is the inverse Fourier transform of the time-varying PSD of the output voltage response using equation (32).

The results from first three case studies clearly demonstrate that the proposed framework can achieve stochastic quantification of the variation in harvestable electric power when the amplitude and driving frequency randomly change

with time. We note that the realistic vibrations of most practical engineered systems fit within the aforementioned case studies in terms of significant randomness of amplitude and driving frequency. Thus, the proposed framework has potential for wide applications in real-world settings.

The main contributions of the proposed framework are two-fold: (i) it is the first attempt to apply a statistical time–frequency analysis to electric power quantification of a piezoelectric energy harvester under non-stationary random vibrations, and (ii) it provides visualization of harvestable electric power based on the ambient vibration data acquired from engineered systems. Through statistical time–frequency analysis, the proposed framework enables the electromechanically-coupled analytical model to deal with the time-variant random nature in a stochastic manner. As a result, it is possible to conduct design optimization of a piezoelectric energy harvester for reliable scavenging of electric power while considering the random nature of vibration. Furthermore, the framework can be used to quickly confirm whether or not it is feasible to operate wireless sensor networks for structural health monitoring or building automation under given vibration conditions.

There can be two main sources of error in stochastic quantification of harvestable electric power. From the standpoint of signal processing, a bias can occur due to the time averages or a trade-off between interference and localization due to the smoothing. Therefore, the size and shape of the smoothing kernel function, as well as the kind of time–frequency representation, should be carefully chosen so as to be appropriate for a given vibration condition. On the other hand, simplification of assumptions can introduce error due to modeling uncertainty in an electromechanical model (e.g., boundary conditions and their interactions). However, these sources of uncertainty can be minimized by model verification and validation (V&V).

In this study, we considered the random nature of given vibration conditions in stochastic quantification of electric power. To investigate the effect of physical uncertainty in a piezoelectric energy harvester itself on the variation of harvestable electric power, future work will combine our results from this study with statistical data for mechanical properties (elastic modulus, density, geometry) and electrical properties (piezoelectric strain coefficient and dielectric permittivity). In addition, statistical model calibration will be incorporated with this study to improve the predictive capability of the analytical model. Future work will also include examination of practical application of the proposed framework to realistic vibration data from engineered systems (e.g., automotive vehicles or power plants).

Acknowledgments

This research was supported by the Fusion Research Program for Green Technologies through the National Research Foundation of Korea (NRF) funded by the Ministry of Science, ICT and Future Planning (NRF-2010-0019092) and the Brain Korea 21 Plus Project in 2013.

References

[1] Sodano H A, Inman D J and Park G 2004 A review of power harvesting from vibration using piezoelectric materials *Shock Vib. Dig.* **36** 197–206

[2] Beeby S P, Tudor M J and White N M 2006 Energy harvesting vibration sources for microsystems applications *Meas. Sci. Technol.* **17** R175–95

[3] Anton S R and Sodano H A 2007 A review of power harvesting using piezoelectric materials (2003–2006) *Smart Mater. Struct.* **16** R1

[4] Beeby S, Tudor M, Torah R, Roberts S, O'Donnell T and Roy S 2007 Experimental comparison of macro and micro scale electromagnetic vibration powered generators *Microsyst. Technol.* **13** 1647–53

[5] Beeby S P, Torah R, Tudor M, Glynne-Jones P, O'Donnell T, Saha C and Roy S 2007 A micro electromagnetic generator for vibration energy harvesting *J. Micromech. Microeng.* **17** 1257

[6] Torres E O and Rincón-Mora G A 2009 Electrostatic energy-harvesting and battery-charging CMOS system prototype *IEEE Trans. Circuits Syst.* I **56** 1938–48

[7] Lallart M, Pruvost S and Guyomar D 2011 Electrostatic energy harvesting enhancement using variable equivalent permittivity *Phys. Lett.* A **375** 3921–4

[8] Wang L and Yuan F 2008 Vibration energy harvesting by magnetostrictive material *Smart Mater. Struct.* **17** 045009

[9] Adly A, Davino D, Giustiniani A and Visone C 2010 Experimental tests of a magnetostrictive energy harvesting device toward its modeling *J. Appl. Phys.* **107** 09A935

[10] Lee S, Youn B D and Jung B C 2009 Robust segment-type energy harvester and its application to a wireless sensor *Smart Mater. Struct.* **18** 095021

[11] Chen X, Xu S, Yao N and Shi Y 2010 1.6 V nanogenerator for mechanical energy harvesting using PZT nanofibers *Nano Lett.* **10** 2133–7

[12] Qi Y, Jafferis N T, Lyons K Jr, Lee C M, Ahmad H and McAlpine M C 2010 Piezoelectric ribbons printed onto rubber for flexible energy conversion *Nano Lett.* **10** 524–8

[13] Qi Y, Kim J, Nguyen T D, Lisko B, Purohit P K and McAlpine M C 2011 Enhanced piezoelectricity and stretchability in energy harvesting devices fabricated from buckled PZT ribbons *Nano Lett.* **11** 1331–6

[14] Ottman G K, Hofmann H F and Lesieutre G A 2003 Optimized piezoelectric energy harvesting circuit using step-down converter in discontinuous conduction mode *IEEE Trans. Power Electron.* **18** 696–703

[15] Guan M and Liao W 2007 On the efficiencies of piezoelectric energy harvesting circuits towards storage device voltages *Smart Mater. Struct.* **16** 498

[16] Roundy S, Leland E S, Baker J, Carleton E, Reilly E, Lai E, Otis B, Rabaey J M, Wright P K and Sundararajan V 2005 Improving power output for vibration-based energy scavengers *IEEE Pervasive Comput.* **4** 28–36

[17] Goldschmidtboeing F and Woias P 2008 Characterization of different beam shapes for piezoelectric energy harvesting *J. Micromech. Microeng.* **18** 104013

[18] Rupp C J, Evgrafov A, Maute K and Dunn M L 2009 Design of piezoelectric energy harvesting systems: a topology optimization approach based on multilayer plates and shells *J. Intell. Mater. Syst. Struct.* **20** 1923–39

[19] Kim M, Hong S, Miller D J, Dugundji J and Wardle B L 2011 Size effect of flexible proof mass on the mechanical

behavior of micron-scale cantilevers for energy harvesting applications *Appl. Phys. Lett.* **99** 243506
[20] Cottone F, Vocca H and Gammaitoni L 2009 Nonlinear energy harvesting *Phys. Rev. Lett.* **102** 080601
[21] Erturk A and Inman D J 2011 Broadband piezoelectric power generation on high-energy orbits of the bistable Duffing oscillator with electromechanical coupling *J. Sound Vib.* **330** 2339–53
[22] Harne R L and Wang K W 2013 A review of the recent research on vibration energy harvesting via bistable systems *Smart Mater. Struct.* **22** 023001
[23] Lallart M, Anton S R and Inman D J 2010 Frequency self-tuning scheme for broadband vibration energy harvesting *J. Intell. Mater. Syst. Struct.* **21** 897–906
[24] Al-Ashtari W, Hunstig M, Hemsel T and Sextro W 2012 Frequency tuning of piezoelectric energy harvesters by magnetic force *Smart Mater. Struct.* **21** 035019
[25] Qi S, Shuttleworth R, Oyadiji S O and Wright J 2010 Design of a multiresonant beam for broadband piezoelectric energy harvesting *Smart Mater. Struct.* **19** 094009
[26] Erturk A, Tarazaga P A, Farmer J R and Inman D J 2009 Effect of strain nodes and electrode configuration on piezoelectric energy harvesting from cantilevered beams *J. Vib. Acoust.* **131** 011010
[27] Lee S and Youn B D 2011 A new piezoelectric energy harvesting design concept: multimodal energy harvesting skin *IEEE Trans. Ultrason. Ferroelectr. Freq. Control* **58** 629–45
[28] Lee S and Youn B D 2011 A design and experimental verification methodology for an energy harvester skin structure *Smart Mater. Struct.* **20** 057001
[29] Roundy S and Wright P K 2004 A piezoelectric vibration based generator for wireless electronics *Smart Mater. Struct.* **13** 1131
[30] Sodano H A, Park G and Inman D 2004 Estimation of electric charge output for piezoelectric energy harvesting *Strain* **40** 49–58
[31] Erturk A and Inman D J 2008 On mechanical modeling of cantilevered piezoelectric vibration energy harvesters *J. Intell. Mater. Syst. Struct.* **19** 1311–25
[32] Dutoit N E and Wardle B L 2007 Experimental verification of models for microfabricated piezoelectric vibration energy harvesters *AIAA J.* **45** 1126–37
[33] Kim M, Hoegen M, Dugundji J and Wardle B L 2010 Modeling and experimental verification of proof mass effects on vibration energy harvester performance *Smart Mater. Struct.* **19** 045023
[34] Erturk A and Inman D J 2009 An experimentally validated bimorph cantilever model for piezoelectric energy harvesting from base excitations *Smart Mater. Struct.* **18** 025009
[35] Halvorsen E 2008 Energy harvesters driven by broadband random vibrations *J. Microelectromech. Syst.* **17** 1061–71
[36] Adhikari S, Friswell M and Inman D 2009 Piezoelectric energy harvesting from broadband random vibrations *Smart Mater. Struct.* **18** 115005
[37] Seuaciuc-Osório T and Daqaq M F 2010 Energy harvesting under excitations of time-varying frequency *J. Sound Vib.* **329** 2497–515
[38] Ali S, Adhikari S, Friswell M and Narayanan S 2011 The analysis of piezomagnetoelastic energy harvesters under broadband random excitations *J. Appl. Phys.* **109** 074904
[39] Zhao S and Erturk A 2012 Electroelastic modeling and experimental validations of piezoelectric energy harvesting from broadband random vibrations of cantilevered bimorphs *Smart Mater. Struct.* **22** 015002
[40] Ikeda T 1996 *Fundamentals of Piezoelectricity* (Oxford: Oxford University Press)
[41] Standards Committee of the IEEE Ultrasonics, Ferroelectrics and Frequency Control Society 1988 *IEEE Standard on Piezoelectricity: An American National Standard* (New York: Institute of Electrical and Electronics Engineers, Inc.)
[42] Holland R and EerNisse E P 1969 *Design of Resonant Piezoelectric Devices* (Cambridge, MA: MIT Press)
[43] Ballas R G 2007 *Piezoelectric Multilayer Beam Bending Actuators: Static and Dynamic Behavior and Aspects of Sensor Integration* (Berlin: Springer)
[44] Gubner J A 2006 *Probability and Random Processes for Electrical and Computer Engineers* (Cambridge: Cambridge University Press)
[45] Meirovitch L 2001 *Fundamentals of Vibrations* (New York: McGraw-Hill)
[46] Shin K and Hammond P J 2008 *Fundamentals of Signal Processing for Sound and Vibration Engineers* (New York: Wiley)
[47] Boashash B 2003 *Time Frequency Signal Analysis and Processing: A Comprehensive Reference* (Amsterdam: Elsevier)
[48] Newland D E 2012 *An Introduction to Random Vibrations, Spectral and Wavelet Analysis* (New York: Dover)
[49] Zhang L, Xiong G, Liu H, Zou H and Guo W 2010 Time–frequency representation based on time-varying autoregressive model with applications to non-stationary rotor vibration analysis *Sadhana* **35** 215–32
[50] Harris C M and Piersol A G 2002 *Harris' Shock and Vibration Handbook* (New York: McGraw-Hill)
[51] Poulimenos A and Fassois S 2006 Parametric time-domain methods for non-stationary random vibration modelling and analysis—a critical survey and comparison *Mech. Syst. Signal Process.* **20** 763–816
[52] Besson O and Castanié F 1993 On estimating the frequency of a sinusoid in autoregressive multiplicative noise *IEEE Trans. Signal Process.* **30** 65–83
[53] Baillie D C and Mathew J 1996 A comparison of autoregressive modeling techniques for fault diagnosis of rolling element bearings *Mech. Syst. Signal Process.* **10** 1–17
[54] Wang W Y and Wong A K 2002 Autoregressive model-based gear fault diagnosis *Trans. ASME J. Vib. Acoust.* **124** 172–9
[55] Zhan Y and Jardine A 2005 Adaptive autoregressive modeling of non-stationary vibration signals under distinct gear states. Part 1: modeling *J. Sound Vib.* **286** 429–50
[56] Braun S 2011 The synchronous (time domain) average revisited *Mech. Syst. Signal Process.* **25** 1087–102
[57] Petsounis K A and Fassois S D 2000 Non-stationary functional series TARMA vibration modelling and analysis in a planar manipulator *J. Sound Vib.* **231** 1355–76
[58] Pham H T and Yang B S 2010 Estimation and forecasting of machine health condition using ARMA/GARCH model *Mech. Syst. Signal Process.* **24** 546–58
[59] Loutridis S J 2004 Damage detection in gear systems using empirical mode decomposition *Eng. Struct.* **26** 1833–41
[60] Parey A, El Badaoui M, Guillet F and Tandon N 2006 Dynamic modelling of spur gear pair and application of empirical mode decomposition-based statistical analysis for early detection of localized tooth defect *J. Sound Vib.* **294** 547–61

[61] Gao Q, Duan C, Fan H and Meng Q 2008 Rotating machine fault diagnosis using empirical mode decomposition *Mech. Syst. Signal Process.* **22** 1072–81
[62] Feldman M 2011 *Hilbert Transform Applications in Mechanical Vibration* (New York: Wiley)
[63] Molla M K I and Hirose K 2010 Hilbert spectrum in time–frequency representation of audio signals considering disjoint orthogonality *Adv. Adapt. Data Anal.* **2** 313–36
[64] Flandrin P 1998 *Time–Frequency/Time-Scale Analysis* (Amsterdam: Elsevier)
[65] Xiao J and Flandrin P 2007 Multitaper time–frequency reassignment for nonstationary spectrum estimation and chirp enhancement *IEEE Trans. Signal Process.* **55** 2851–60
[66] Flandrin P, Auger F and Chassande-Mottin E 2003 Time–frequency reassignment: from principles to algorithms *Applications in Time–Frequency Signal Processing* ed A Papandreou-Suppappola (Boca Raton, FL: CRC) chapter 5, pp 179–203
[67] NI Developer Zone The Fundamentals of FFT-Based Signal Analysis and Measurement in LabVIEW and LabWindows/CVI (Online), available from: www.ni.com/white-paper/4278/en#toc3
[68] Li J and Chen J 2009 *Stochastic Dynamics of Structures* (New York: Wiley)
[69] Rao S S 2007 *Vibration of Continuous Systems* (New York: Wiley)
[70] Haug E and Choi K K 1993 *Methods of Engineering Mathematics* (Englewood Cliffs, NJ: Prentice-Hall)
[71] Erturk A and Inman D J 2011 *Piezoelectric Energy Harvesting* (New York: Wiley)
[72] Youn B D, Choi K K, Du L and Gorsich D 2007 Integration of possibility-based optimization and robust design for epistemic uncertainty *J. Mech. Des.* **129** 876–82
[73] Youn B D and Xi Z M 2009 Reliability-based robust design optimization using the eigenvector dimension reduction (EDR) method *Struct. Multidiscip. Optim.* **37** 475–92
[74] Hu C and Youn B D 2011 Adaptive-sparse polynomial chaos expansion for reliability analysis and design of complex engineering systems *Struct. Multidiscip. Optim.* **43** 419–42
[75] Liu S C 1971 Time-varying spectra and linear transformation *Bell Syst. Tech. J.* **50** 2365–74
[76] Engineering Fundamentals Inc. IHS GlobalSpec (Online), available from: www.efunda.com/materials/piezo/material_data/matdata_output.cfm?Material_ID=PZT-5H